

Monolithic integration of enhancement-mode vertical driving transistor on a standard InGaN/GaN light emitting diode structure

Xing Lu, Chao Liu, Huaxing Jiang, Xinbo Zou, Anping Zhang, and Kei May Lau

Citation: [Applied Physics Letters](#) **109**, 053504 (2016); doi: 10.1063/1.4960105

View online: <http://dx.doi.org/10.1063/1.4960105>

View Table of Contents: <http://scitation.aip.org/content/aip/journal/apl/109/5?ver=pdfcov>

Published by the [AIP Publishing](#)

Articles you may be interested in

[Nano-light-emitting-diodes based on InGaN mesoscopic structures for energy saving optoelectronics](#)

Appl. Phys. Lett. **109**, 041103 (2016); 10.1063/1.4960007

[Effect of the band structure of InGaN/GaN quantum well on the surface plasmon enhanced light-emitting diodes](#)

J. Appl. Phys. **116**, 013101 (2014); 10.1063/1.4886223

[Optimization of InGaN/GaN superlattice structures for high-efficiency vertical blue light-emitting diodes](#)

J. Appl. Phys. **114**, 173101 (2013); 10.1063/1.4828488

[Influence of laser lift-off on optical and structural properties of InGaN/GaN vertical blue light emitting diodes](#)

AIP Advances **2**, 022122 (2012); 10.1063/1.4717493

[GaN micro-light-emitting diode arrays with monolithically integrated sapphire microlenses](#)

Appl. Phys. Lett. **84**, 2253 (2004); 10.1063/1.1690876

The banner features a blue background with a molecular structure of spheres and sticks on the left. On the right, the text 'NEW Special Topic Sections' is written in large, white, sans-serif font. Below this, the text 'NOW ONLINE' is in yellow, followed by 'Lithium Niobate Properties and Applications: Reviews of Emerging Trends' in white. The AIP Applied Physics Reviews logo is in the bottom right corner. On the left side of the banner, there is a small inset image of the journal cover for Applied Physics Reviews, showing a diagram of a device structure.

Monolithic integration of enhancement-mode vertical driving transistors on a standard InGaN/GaN light emitting diode structure

Xing Lu,^{1,a)} Chao Liu,² Huaxing Jiang,² Xinbo Zou,² Anping Zhang,¹ and Kei May Lau²

¹State Key Laboratory of Electrical Insulation and Power Equipment, Xi'an Jiaotong University, Xi'an 710049, People's Republic of China

²Department of Electronic and Computer Engineering, Hong Kong University of Science and Technology, Clear Water Bay, Kowloon, Hong Kong

(Received 16 May 2016; accepted 19 July 2016; published online 2 August 2016)

In this letter, monolithic integration of InGaN/GaN light emitting diodes (LEDs) with vertical metal-oxide-semiconductor field effect transistor (VMOSFET) drivers have been proposed and demonstrated. The VMOSFET was achieved by simply regrowing a p- and n-GaN bilayer on top of a standard LED structure. After fabrication, the VMOSFET is connected with the LED through the conductive n-GaN layer, with no need of extra metal interconnections. The junction-based VMOSFET is inherently an enhancement-mode (E-mode) device with a threshold voltage of 1.6 V. By controlling the gate bias of the VMOSFET, the light intensity emitted from the integrated VMOSFET-LED device could be well modulated, which shows great potential for various applications, including solid-state lighting, micro-displays, and visible light communications. *Published by AIP Publishing.* [<http://dx.doi.org/10.1063/1.4960105>]

InGaN/GaN light emitting diodes (LEDs) have been used extensively in backlight units, automobiles and general illumination due to their high luminous efficacy and extremely long lifetime compared to traditional light sources.^{1,2} Meanwhile, GaN-based transistors for power switching and RF applications have received remarkable research interests in recent years because of their superior properties, such as large breakdown voltage, fast operating speed, low power loss, and high temperature duration.^{3–5} Sharing a common material platform, GaN-based LEDs and on-chip driving electronics can be monolithically integrated to yield a compact smart-lighting system, potentially for many applications such as solid-state lighting, micro-displays, and visible light communications (VLCs).^{6–8} The advantages include improved performance, enhanced reliability, reduced form factor, and parasitics, leading to lower overall cost.

Previously, monolithic integration of GaN-based LEDs with on-chip driving transistors was demonstrated by our group⁹ and others^{10,11} using either selective epi growth (SEG) or selective epitaxial removal (SER) methods. However, in those integration schemes, the transistors were mostly depletion-mode (D-mode) devices with lateral configurations. In practical applications, enhancement-mode (E-mode) transistors are always preferred, because they can simplify the driving circuits with a single-polarity voltage supply and improve the reliability of the whole system. Very recently, vertical metal-oxide-semiconductor field effect transistors (VMOSFETs) with high breakdown voltage and low specific on-resistance ($R_{on,sp}$) have been demonstrated using a free-standing GaN substrate for power switching applications.^{12–14} These VMOSFETs are typically E-mode devices. Moreover, when compared with lateral devices, VMOSFETs are more suitable for integration with LEDs since they share similar junction-based vertical structures.

In this letter, we demonstrate the monolithic integration of InGaN/GaN LEDs with vertical driving MOSFETs. By regrowing a simple p- and n-GaN bilayer on top of the standard LED diode structure, an n/p/n structure was formed for VMOSFET fabrication. The demonstrated VMOSFET features a relatively high positive threshold voltage of 1.6 V. The serially connected VMOSFET-LED device emits blue light that can be efficiently modulated by gate biasing of the VMOSFET. This integrated device offers an alternate choice for potential future deployment of integrated miniature smart-lighting systems.

Fig. 1 depicts the cross-sectional schematic of the integrated VMOSFET-LED device. To start with, a standard LED diode structure was grown on a 2-in. sapphire substrate in an Aixtron 2400HT metal organic chemical vapor deposition (MOCVD) system. The standard LED consisted of a 2.0 μm unintentionally doped GaN layer, a 2.0 μm n-GaN layer with a Si dopant concentration of around $5 \times 10^{18} \text{ cm}^{-3}$, five periods of InGaN/GaN multiple quantum wells (MQWs) with 3 nm-thick wells and 11 nm-thick barriers, a 15 nm p-Al_{0.15}Ga_{0.85}N layer, and a 130 nm p-type GaN layer with a

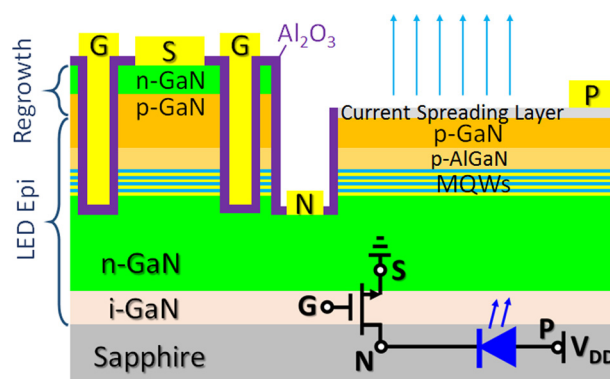


FIG. 1. Schematic cross section of the monolithically integrated GaN-based LED with a circular-gate VMOSFET.

^{a)}Email: eexlu@connect.ust.hk. Tel.: (86) 29 82664008.

Mg dopant concentration of around $3 \times 10^{19} \text{ cm}^{-3}$. To create a regrowth mask, 200 nm SiO_2 was deposited on the LED wafer by plasma enhanced chemical vapor deposition (PECVD) and then patterned using buffered oxide etchant (BOE). The regrowth mask covered half of the 2-in. LED wafer. Afterwards, the regrowth of a p- and n-GaN bilayer was carried out on the exposed region to form an n/p/n structure for the VMOSFETs. Trimethylgallium (TMGa) and ammonia (NH_3) were used as precursors for Ga and N, respectively. The p-GaN layer was 370 nm thick with a Mg dopant concentration of around $3 \times 10^{19} \text{ cm}^{-3}$, while the 200 nm n-GaN layer had a two-step doping profile (Si dopant concentration: $\sim 1 \times 10^{19} \text{ cm}^{-3}$ for the first 180 nm and up to $5 \times 10^{19} \text{ cm}^{-3}$ for the remaining 20 nm). After regrowth, the total thickness of the p-GaN layer was 500 nm. Atomic force microscopy (AFM) was carried out to investigate the surface morphology evolution. Fig. 2 shows the AFM images of the sample before and after regrowth with a scanned area of $10 \times 10 \mu\text{m}^2$. The root mean square (RMS) roughness was 5.8 nm for the as-grown LED surface, while it was reduced to 0.8 nm after regrowth of the bilayer GaN and well-aligned step flow patterns were observed. The improved surface morphology was mainly attributed to the alleviated growth temperature, from 985°C for p-GaN to 1080°C for n-GaN. Higher temperature increased the Ga atoms' diffusion length during the growth, leading to smoother surface morphology. Fig. 3 compares the normalized photoluminescence (PL) spectra measured from exactly the same region of the LED

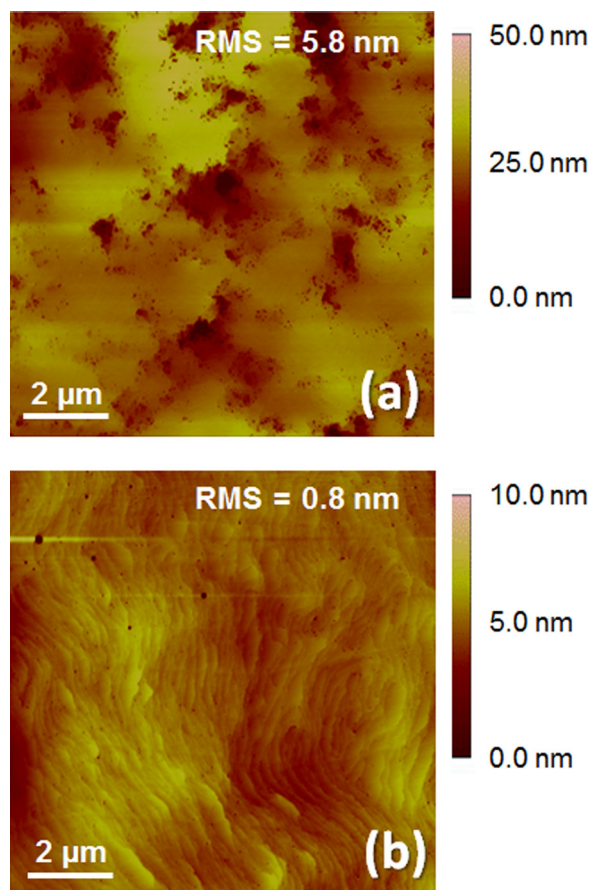


FIG. 2. Surface morphology of the LED sample (a) before and (b) after regrowth of the bilayer GaN.

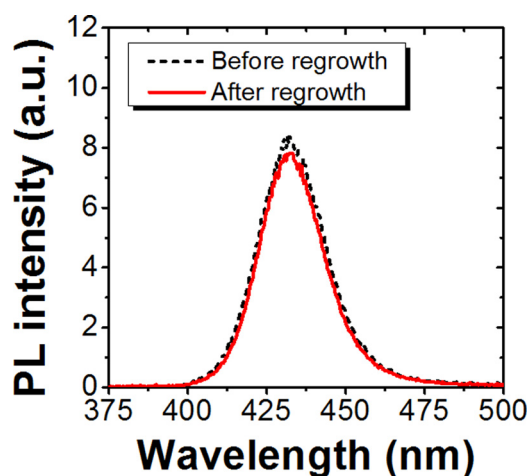


FIG. 3. PL spectra of the LED sample before and after regrowth of the bilayer GaN.

part on the wafer before and after regrowth, where the SiO_2 regrowth mask was completely removed using BOE. The PL peak intensity was only decreased by about 7% after the regrowth, indicating no significant degradation in optical properties of the LED's MQWs.

After completely removing the SiO_2 regrowth mask by BOE, mesa isolation etching for both the LEDs and VMOSFETs was performed using a Cl_2 -based inductively coupled plasma (ICP) etch. Then, gate trenches for the VMOSFETs were created by ICP etch. After that, a rapid thermal annealing (RTA) was performed at 800°C for 1 min in a N_2 ambient to activate the p-GaN layer, resulting in a hole concentration of around $1 \times 10^{17} \text{ cm}^{-3}$. A 50 nm Al_2O_3 was then blanket deposited by atomic layer deposition (ALD), serving as the gate dielectric for the VMOSFETs. After selective removal of the Al_2O_3 in the LED region, a current spreading layer was formed by e-beam evaporation of Ni/Au metal followed by RTA in an atmospheric ambient at 570°C for 5 min.¹⁵ Subsequently, a multi-layer metal stack Cr/Al/Ti/Au was evaporated, after opening the contact holes by BOE, to form both the n-electrodes for the LEDs and the source Ohmic contacts for the VMOSFETs. Finally, the Ni/Au gate metal for the VMOSFETs was deposited.

As shown in Fig. 1, the connection between the LED and VMOSFET was realized by sharing the highly doped bottom n-GaN layer. It was found that metal-to-GaN contact resistances dominate the overall parasitic resistance of the interconnection between the integrated LED and transistor.¹⁶ Therefore, a significant reduction in parasitic resistance is expected using the same scheme in this study by eliminating the extra metal interconnections. In addition, due to the elimination of two metal-to-GaN contacts between the LED and VMOSFET, the chip area could potentially be saved. Fig. 4 shows an optical micrograph of the fabricated monolithic VMOSFET-LED device that emitted blue light, with its circuit diagram shown in the inset. The circular shaped LED exhibited a good uniformity of light emission with a wavelength of around 430 nm. The LED's n-electrode also serves as the drain electrode for the VMOSFET, so the LED and VMOSFET could be characterized separately.

Fig. 5 compares the I-V and light output power (LOP) characteristics of the integrated and stand-alone reference

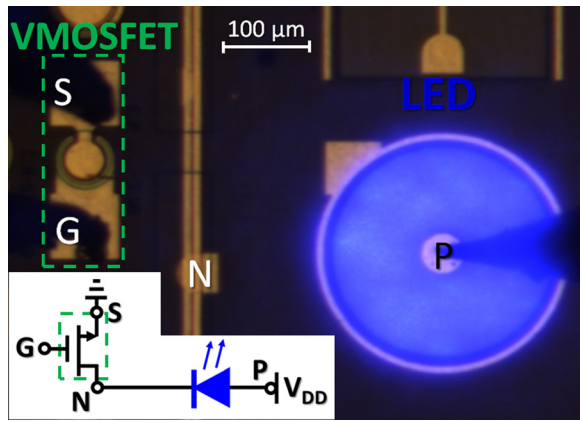


FIG. 4. Optical micrograph of the monolithically integrated VMOSFET-LED device. The inset shows the equivalent circuit diagram.

LEDs. The diameter of the LED mesa is $300\ \mu\text{m}$. When compared with the stand-alone reference LED that was from another individual LED chip fabricated using an identical epitaxial structure and a standard LED process, no obvious performance degradation was found in the integrated one, suggesting the high compatibility of the integration process in our study.

The output characteristics of the individual VMOSFET and the integrated VMOSFET-LED device are plotted in Fig. 6. The threshold voltage of the fabricated VMOSFET

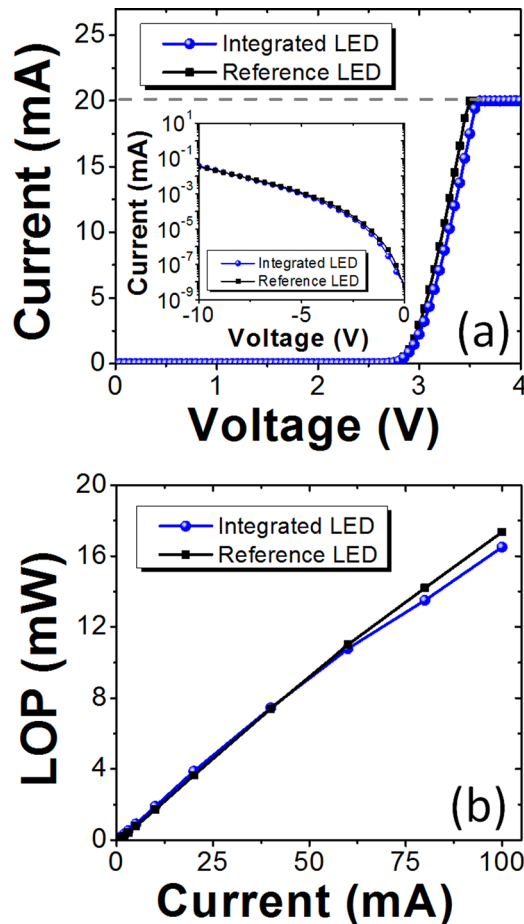


FIG. 5. Comparison of the (a) I-V and (b) LOP characteristics between the integrated and stand-alone reference LEDs. The inset compares the reverse leakage currents.

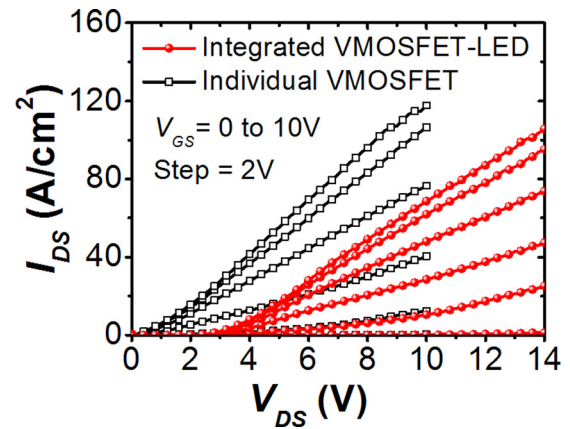


FIG. 6. Output characteristics of the individual VMOSFET and the integrated VMOSFET-LED device.

was $+1.6\ \text{V}$. The maximum output current density of the VMOSFET was $118\ \text{A}/\text{cm}^2$ at $V_{DS} = 10\ \text{V}$ and $V_{GS} = 10\ \text{V}$. The I-V curve of the integrated VMOSFET-LED device (measured between the S and P nodes in Fig. 1) shifted towards a positive voltage by around $3\ \text{V}$ compared with that of the individual VMOSFET, which resulted from the turn-on voltage of the serially connected LED. The non-saturated drain current could be explained by the low hole concentration of the thin p-GaN channel layer ($\sim 500\ \text{nm}$), which was easy to deplete due to the highly doped n-GaN drain layer underneath. This phenomenon could be mitigated by inserting a layer of less-doped n-GaN between the MQWs and the bottom n-GaN layer to modify the junction as has been done in LED technology.¹⁷ Correspondingly, the blocking capability of the VMOSFET would be enhanced as well.

The VMOSFET in this work showed a relatively low output current density, as compared to the reported results in the literature.^{12,13} It is worth noting that our VMOSFET layout is circular in shape, with a diameter of $37\ \mu\text{m}$. This layout had a relatively low channel density, i.e., the ratio of gate width to device area (W_g/S), of only around $0.045\ \mu\text{m}^{-1}$ ($193\ \mu\text{m}/4300\ \mu\text{m}^2$), which significantly limited the device output current density. Also, the dry etch induced damage to the side-wall channel might degrade the channel electron mobility and therefore the output current density.¹⁴ Further

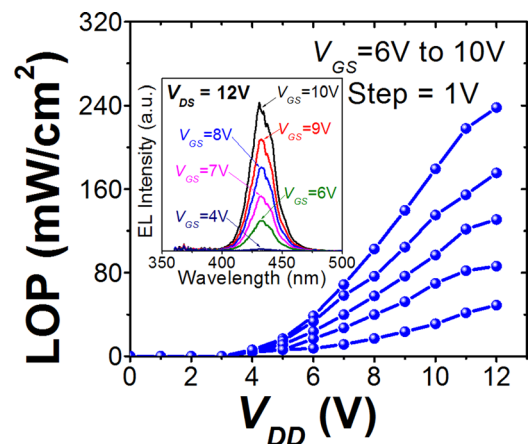


FIG. 7. LOP characteristics of the integrated VMOSFET-LED device with modulated gate biases. The inset shows the EL spectra modulated by gate biasing at $V_{DS} = 12\ \text{V}$.

improvement of the output current density for the integrated VMOSFETs could be achieved by optimizing the device layout and trench etching techniques. Using polygonal cells to increase the channel density and a tetramethylammonium hydride (TMAH) wet etching to smoothen the channel surface as suggested in Refs. 13 and 18 are viable options.

With supply voltage (V_{DD}) and gate modulation voltage (V_{GS}) applied to the integrated VMOSFET-LED device, as shown by the circuit configuration in the inset of Fig. 4, the device emitted modulated blue light (~ 430 nm) by gate biasing. Fig. 7 presents the LOP density of the integrated VMOSFET-LED device versus the applied voltage. The electroluminescence (EL) spectra of the integrated device with a fixed V_{DD} but various V_{GS} are shown in the inset of Fig. 7. It can be seen that the LOP of the integrated LED could be effectively modulated by the gate biasing of the VMOSFET. Nevertheless, in this first demonstration, the channel density of the VMOSFET and the layout of the integrated devices are yet to be optimized. Further improvement is needed in our future mask design.

Monolithic integration of InGaN/GaN LEDs with E-mode vertical driving MOSFETs has been developed based on a standard LED epitaxial structure. The integration approach and the performances of the integrated devices have been described in detail. This work, offering an alternate driving circuit design option, represents a major step toward the development of full-GaN miniature smart-lighting systems for a wide range of applications.

This work was supported in part by the National Natural Science Foundation of China under Grant No. 51507131, the State Key Laboratory of Electrical Insulation and Power Equipment EIPE16302 and the Research Grants Council (RGC) theme-based research scheme (TRS) of the Hong Kong Special Administrative Region Government under Grant No. T23-612/12-R. The experiments were conducted

at the Hong Kong University of Science and Technology. The authors would like to thank Dr. Q. Li, Mr. X. Zhang, and Mr. Y. Cai for valuable discussion, and the staff of the NFF and MCPF of HKUST for technical support.

- ¹E. F. Schubert and J. K. Kim, *Science* **308**(5726), 1274 (2005).
- ²M. H. Crawford, *IEEE J. Sel. Top. Quantum Electron.* **15**, 1028 (2009).
- ³K. Shinohara, D. C. Regan, Y. Tang, A. L. Corrion, D. F. Brown, J. C. Wong, J. F. Robinson, H. H. Fung, A. Schmitz, T. C. Oh *et al.*, *IEEE Trans. Electron Devices* **60**(10), 2982 (2013).
- ⁴M. Kuzuhara and H. Tokuda, *IEEE Trans. Electron Devices* **62**, 405 (2015).
- ⁵X. Lu, J. Ma, H. Jiang, C. Liu, P. Xu, and K. M. Lau, *IEEE Trans. Electron Devices* **62**, 1862 (2015).
- ⁶Z. Li, J. Waldron, T. Detchprohm, C. Wetzel, R. F. Karliceck, and T. P. Chow, *Appl. Phys. Lett.* **102**, 192107 (2013).
- ⁷Z. Liu, W. C. Chong, K. M. Wong, and K. M. Lau, *J. Disp. Technol.* **9**, 678 (2013).
- ⁸J. J. D. McKendry, D. Massoubre, S. Zhang, B. R. Rae, R. P. Green, E. Gu, R. K. Henderson, A. E. Kelly, and M. D. Dawson, *J. Lightwave Technol.* **30**, 61 (2012).
- ⁹Z. Liu, T. Huang, J. Ma, C. Liu, and K. M. Lau, *IEEE Electron Device Lett.* **35**, 330 (2014).
- ¹⁰F. G. Kalaitzakis, E. Iliopoulos, G. Konstantinidis, and N. T. Pelekanos, *Microelectron. Eng.* **90**, 33 (2012).
- ¹¹Y. J. Lee, Z. P. Yang, P. G. Chen, Y. A. Hsieh, Y. C. Yao, M. H. Liao, M. H. Wang, and J. M. Hwang, *Opt. Express* **22**, A1589 (2014).
- ¹²T. Kachi, in *2015 IEEE International Electron Devices Meeting (IEDM)* (2015), p. 16.1.1.
- ¹³O. Tohru, I. Tsutomu, U. Yukihiisa, and N. Junya, *Appl. Phys. Express* **8**, 054101 (2015).
- ¹⁴H. Otake, K. Chikamatsu, A. Yamaguchi, T. Fujishima, and H. Ohta, *Appl. Phys. Express* **1**, 011105 (2008).
- ¹⁵K. M. Lau, K. M. Wong, X. Zou, and P. Chen, *Opt. Express* **19**, A956 (2011).
- ¹⁶C. Liu, Y. Cai, Z. Liu, J. Ma, and K. M. Lau, *Appl. Phys. Lett.* **106**, 181110 (2015).
- ¹⁷J. Cho, A. Mao, J. K. Kim, J. K. Son, Y. Park, and E. F. Schubert, *Electron. Lett.* **46**, 156 (2010).
- ¹⁸M. Kodama, M. Sugimoto, E. Hayashi, N. Soejima, O. Ishiguro, M. Kanechika, K. Itoh, H. Ueda, T. Uesugi, and T. Kachi, *Appl. Phys. Express* **1**, 021104 (2008).